

Safety zone in an entertainment park: envelopes and Maltese Cross related to an offset of an astroid

Thierry Dana-Picard,

ndp@jct.ac.il,

Jerusalem College of Technology

Havaad Haleumi St. 21, Jerusalem 9116011

Israel

Abstract

There exist different, non totally equivalent, definitions of an envelope of a parameterized family of plane curves. Using software, it is possible to explore the different approaches, either via geometric constructions and automated commands or using analytic methods. In this paper, we explore examples using joint work with a Dynamic Geometry System (DGS) and a Computer Algebra System (CAS). Each package provides its own contributions, and together they contribute to the exploration, to obtain parametric presentations and implicit equations on the one hand, and to have benefit of automatic animations and mouse-driven dynamic work on the other hand. Zooming and increasing precision of approximations are crucial. We study an envelope of a family of circles centered on an astroid, i.e. an offset of this astroid, and explore its physical meaning to determine a safety zone of a concrete tourist attraction in an entertainment park. Among other results, a new construction of a Maltese Cross is obtained.

1 Introduction

Packages for Dynamic Geometry (generally called DGS, for Dynamic Geometry Systems) have been developed along the last decades, as technological tools enabling direct manipulation and visualization of all the objects of plane geometry (later developments exist for 3D geometry). These packages enable to modify directly figures and configurations, either by dragging points with the mouse, or using a slider bar. At the beginning, Laborde noted in [23] that a DGS "was mainly used as an amplifier for visualizing properties, but not really the source of the task given to the students, nor as a tool for solving the task". Since then, the situation has changed, together with the increase of DGS abilities. New teaching practices, using these tools, have been documented and analyzed by Gueudet and Trouche in [19].

Because of its interactive abilities, DGS took an always-growing place, both in classroom and in lab, for exploration, discovery and research. A DGS is an efficient tool for conjecture and discovery of new theorems. For example, after having drawn a triangle and its heights,

dragging one of the vertices enables to visualize that the heights always intersect at a single point. This does not replace a proof, but actually provides infinitely many examples in a few seconds.

The introduction of automated methods for exploration and derivation of new theorems have been analysed and documented in [5, 6, 7]. Beginning with Wu's work in the 1980's [35, 36, 37], new algorithms have been implemented, opening new fields of research, such as automatic proof and automatic discovery. Recio and Velez say [28]: "While automatic proving deals with verifying geometric statements, automatic discovery tries to find complementary hypotheses for statements to become true or ... to finding the missing hypotheses so that a given conclusion follows from a given incomplete set of hypotheses".

The automated determination of loci has been made possible: GeoGebra's commands **Locus** and **LocusEquation** are now well documented and widely used; see [28, 1, 4]. In the same area, a command **Envelope** has been added, and its advances are also well documented. Kovács reports in [21] that "animations can be performed quickly enough by using today's computers with implicit computer algebra use. In the background, without notifying the user on the fact that thousands of symbolic computations are performed, a pure dynamic geometry experience can be relived, making geometry more geometrical than before". Kovács analyses also the speed of the newly implemented methods and compares them to other implementations for a great number of classical theorems in Geometry. From the user's point of view, the geometric experience and its dynamics are transparent to the huge symbolic and numerical computations needed for them. These computations are the role of the CAS embedded into the DGS; the CAS embedded in GeoGebra is Giac [22]. The DGS allows a fine exploration because of its well-developed zooming abilities, which re-compute the needed data in real time. This, together with improving the precision of the approximations, reveal new properties of the curves under study.

Nevertheless, it may be important to use another CAS, offering features which the embedded CAS has not. The two kinds of software can have some form of dialog, which is described and analyzed in [18]. As of today, this dialog exists via the user, who transfers manually (using copy-paste) output of one kind of software as input for work with the second package. The example studied in the next section has been treated using GeoGebra with a fruitful dialog with Maple, using extensively the last's symbolic abilities. This DGS-CAS dialog is still in his infancy; we hope that the next future will bring developments enabling automatic dialog between packages.

A large part of the work here is made using trigonometric parametrizations for curves, and not rational parametrizations, although these exist. One of the reasons is the efficiency of the animations which are constructed. A comparison appears at the end of the paper.

2 Envelopes and offsets

Already in 1962, Thom [34] complains that envelopes disappeared from the standard curriculum¹, despite their numerous applications, e.g. in Engineering (robotics, hydrology, etc.). A

¹At the time Thom wrote his paper, envelopes began not to be taught anymore, in mathematics curriculum, at least in France. The topic is hardly present in textbooks there from the 60's and beyond. Of course, the author of the present paper could not check all of them. A chapter is devoted to envelopes in the textbook by Cagnac et al. [11], in the volume on "Applications of Analysis to Geometry". This book was used by

classical example, for a non-noisy design of gears back to Euler, is described in [33] (pp. 108-109). Among the possible reasons for the disappearance, Thom lists the following ones:

- The classical theory is not rigorous enough.
- There are too many particular cases: fixed points, singular points, stationary curves, etc.
- Nothing ensures that all the “pathological” cases have been included in a catalogue.
- Actually: the theory is so rich that it is impossible to force it into the rules of a rigorous pedagogy.

Nevertheless, envelopes and offsets are still a live domain of research, generally related to applied situations where they may require numerical approximations (see [27, 31]). Envelopes knew a revival among mathematicians working in another direction (in Spain, Austria, Israel, etc.), in particular with the development of automated tools to determine them (see for example [7, 8, 9, 10, 15, 16] and the list is not exhaustive. This revival led eventually to an extension of the curriculum.

Botana and Recio report in [8] on 4 different definitions of an envelope, according to a Wikipedia page:

Definition 1 *Let C_t be a 1-parameter family of curves given by an equation $F(x, y, t) = 0$. The envelope of the family $\{C_t\}$ is the set of all points (x, y) such that there is a t verifying the system of equations*

$$\begin{cases} F(x, y, t) = 0 \\ \frac{\partial F(x, y, t)}{\partial t} = 0 \end{cases} \quad (1)$$

i.e., the envelope is the projection over the (x, y) -plane of the points, in the (x, y, t) -3 dimensional space, belonging to the surface with equation $F(x, y, t) = 0$ and having tangent plane parallel to the t -axis (or being singular points and, thus, not having tangent plane, properly speaking);

Definition 2 *With the same notations as above. The envelope is the set of limit points of intersections of nearby curves C_t .*

Definition 3 *With the same notations as above. The envelope is a curve tangent to all the given curves C_t .*

Definition 4 *The envelope is the curve that bounds the planar region described by the points belonging to the curves C_t in the family.*

Only Def. 1 is mentioned by Berger ([3], sections 9.6.7 and 14.6.1). In [20], Kock distinguishes 3 different definitions of an envelope: *synthetic* (actually Def. 2), *impredicative* (actually Def. 3; there, he emphasizes the uniqueness of the tangency point) and *analytic* (Def. 1). Then he analyzes the problems that each one raises. The impredicative definition is hard to apply, but can be the basis of an activity, in an elementary situation, as shown in [15].

mathematics undergraduates and future engineers. In Berger’s monograph on Geometry [3], envelopes have a quite small place.

Examples of determination of an envelope using Def. 2 can be found in [15] and in [8]. In this last work, Botana and Recio relate to the way software such as Cabri and Cinderella apply this definition to return the envelope as a curve. Note that in Def. 2, the notion of limit points is not well-defined. Nevertheless, [15] shows how to obtain Def. 1 as a theorem from Def. 2.

These definitions do not contain uniqueness of an envelope. More than two disjoint curves can meet the requirements of one of the definitions, each one is an envelope, and their union also. This is illustrated in Section 3. Back to [8], Botana and Recio note that the different definitions express "the existence of a plurality of approaches to the concept of envelope, as well as describing the many subtle and difficult aspects involved in handling this apparently elementary notion" and they discuss the non equivalence of the 4 definitions.

Usage of the automated commands for the determination of loci and envelopes has constraints, related to the underlying algorithms and the kind of input that they request. In [10], Botana and Recio propose a way to consider the dependence of the family on a moving point, rather than on a real parameter. With tools of algebraic geometry, they elaborate on the taxonomy of [1] to distinguish special components, normal components and acceptable component. This is necessary to determine whether an acceptable special component of an envelope is part of the true envelope (with regards to the standard definition #1) or not. In Section 3, we do not use the **Envelope** command of GeoGebra, as the 1-parameter family of curves is determined by equations, and not by geometric constructions from specific points (no tracer, etc.). Therefore, the exploration has to rely strongly on analytic computations.

Def. 1 contains the definition of an offset given in [2] as a particular case.

Definition 5 *The offset of a curve \mathcal{C} at distance d , denoted $\mathcal{O}_d(\mathcal{C})$, is "essentially" the envelope of the family of circles centred at the points of \mathcal{C} with fixed radius d .*

This is a particular case of an envelope in the sense of Def. 4 as noted in [2].

A general description and properties can be found in [2, 29, 30]. In particular, the authors note that an implicit equation of an offset is generally much more complicated than for the original curve. Figure 1 shows two offsets of the ellipse \mathcal{E} whose equation is $\frac{x^2}{16} + \frac{y^2}{4} = 1$, (a) at distance $1/2$ and (b) at distance 2 , obtained with GeoGebra. Each plot shows two components, one external and one internal to the given ellipse. If in the case $d = 1/2$, the offset seems to be the disjoint union of two ellipses parallel to \mathcal{E} (for a precise meaning of "parallel", see op. cit.). In fact, they are not ellipses. For $d = 2$, the internal component seems more complicated. Such curves have been studied in [15].

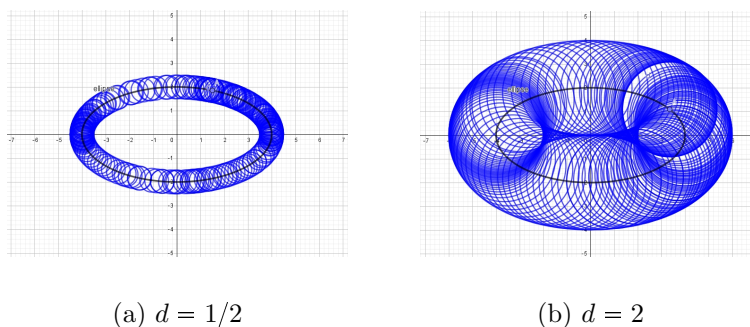


Figure 1: Two offsets of the same ellipse

We will experience the difficulties to determine implicit equations for an offset in Section 4, working mostly with a parametric presentation. We will see also the relation of these notions with the industrial notion of a safety zone. The level of complexity of the equations and formulas will require a heavy usage of DGS-CAS and of approximations.

Section 3 relies on Def. 1 and Def. 4. On the one hand, work is based on the solution of System (1), then on plots and animations of curves given by parametric equations, and not on geometric constructions. On the other hand, a physical interpretation of the output as the borderline of a safety zone seems different from what is expected from Definition #4. Therefore, the notion of an offset is used (see below).

Example of offsets of ellipses have been studied in [13, 15] and some extension towards 3D in [16]. The geometric situation has been explored with a DGS, then translated into equations. Envelopes have been determined by the CAS assisted solution of System (1), providing a parametric representation of the envelope. This yielded a precise plot of the envelope. In order to obtain an implicit equation of the envelope, the equations have been transformed into polynomial equations, using a change of parametrization from trigonometric to rational. Then, the Gröbner bases package of a CAS and the computation of an Elimination Ideal has been performed. For more details, we refer to [12]. We use this method in Section 3. An advanced algorithm, called the Gröbner Cover algorithm, has been developed by Montes [26] and enables to avoid the appearance of irrelevant components. See the discussion in [9].

In previous studies of 1-parameter families of plane curves, the **Trace On** feature enabled to conjecture the existence of an envelope, and even to preview its shape. We used it for Figure 2 in next section, but here it is hard to have a good conjecture regarding the actual shape of an envelope. Actually, this depends on which definition of an envelope is considered. Considering Definition #4, we explore here the offset at distance $1/2$ of the astroid, and study its relations with the safety zone around a physical moving carousel. We discuss that in Section 4.

3 Envelope of a family of circles centred on an astroid

We consider the astroid \mathcal{A} whose implicit equation is $|x|^{2/3} + |y|^{2/3} = 1$. It is displayed in Fig. 2(a). The astroid is a very interesting curve, appearing in various ways. In particular, the isoptics of an astroid have been studied in [13]. The astroid \mathcal{A} has also a simple trigonometric parametrization:

$$\begin{cases} x(t) = \cos^3 t \\ y(t) = \sin^3 t \end{cases}, \quad t \in [0, 2\pi]. \quad (2)$$

Remark 6 *Note that, as sine and cosine can be expressed as rational functions, the astroid \mathcal{A} has also a rational parametrization. We show the corresponding equations in Appendix A, and use them later in the present section.*

Recall that parametric plot is generally more accurate than implicit plot (as explained in [38]), whence a special importance of these parametrizations. This is true for other issues also; for example, the study of bisoptics of an astroid has been performed in [13], using mostly this trigonometric parametrization and other formulas derived from it, such as determination of tangents. An implicit plot has some flaws, no matter which software is used. Therefore, we work here with the parametric presentation given in Equation (2).

Denote by A_t the point of the astroid \mathcal{A} corresponding to the parameter t , and by \mathcal{C}_t the circle centred at A_t and whose radius is equal to $\frac{1}{2}$. An implicit equation for \mathcal{C}_t is $F(x, y, t) = 0$, where:

$$F(x, y, t) = (x - \cos^3 t)^2 + (y - \sin^3 t)^2 - \frac{1}{4}. \quad (3)$$

Fig. 2(b) displays a snapshot of a dynamic exploration.

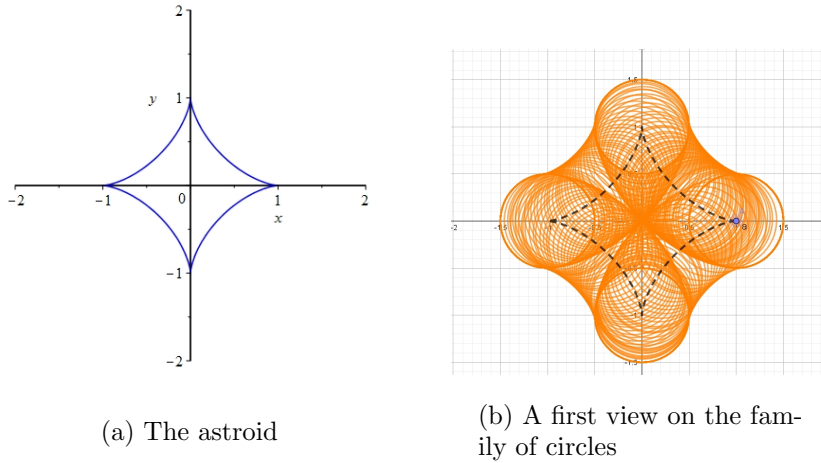


Figure 2: The astroid and the parameterized family of circles

A first conjecture is that an envelope exists in the sense of Def. 4, and is shaped as a rounded cross around all the circles. No valuable other conjecture can still be made because of the "dense" part in the middle of the figure. We switch to analytic work with a CAS.

An envelope of the family of circles $\{\mathcal{C}_t\}$, in the sense of Def. 1, is given by the solutions of the system of equations (1). Here it reads as follows:

$$\begin{cases} (x - \cos^3 t)^2 + (y - \sin^3 t)^2 - \frac{1}{4} = 0 \\ (x - \cos^3 t)^2 \cos^2 t \sin t + (y - \sin^3 t)^2 \sin^2 t \cos t = 0 \end{cases} \quad (4)$$

After simplification, we have:

$$\begin{cases} (x - \cos^3 t)^2 + (y - \sin^3 t)^2 - \frac{1}{4} = 0 \\ \sin 2t(y \sin t - x \cos t + 2 \cos^2 t - 1) = 0 \end{cases} \quad (5)$$

The output of the CAS computations with the **solve** command gives the following solutions for x, y of System 5 (after simplification):

$$\begin{cases} x = \cos^3 t + \frac{1}{2} |\sin t| \\ y = -\frac{1}{2 \sin t} (4 \cos^2 t - \cos t (2 \cos^3 t + |\sin t|)) \end{cases} \quad (6)$$

and

$$\begin{cases} x = \cos^3 t - \frac{1}{2} |\sin t| \\ y = -\frac{1}{2 \sin t} (4 \cos^2 t - \cos t (2 \cos^3 t + |\sin t|)) \end{cases} \quad (7)$$

Note the symmetry about the y -axis between the two curves. Each of these parametrizations defines an envelope of the given family of circles, and the union of both is also an envelope of this family. Separate plots of these components are displayed in Fig. 3. Note that the two components are open curves.

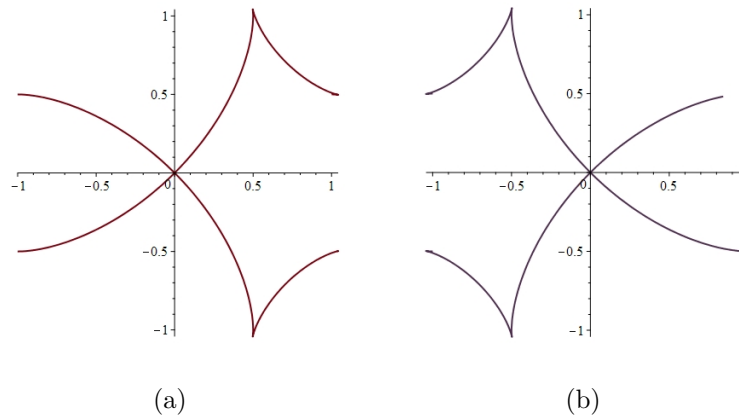


Figure 3: Two envelopes of a parametric family of circles

Fig. 4 shows the union of the components together with the given astroid. The union of the two components can also be viewed as the union of two non smooth loops.

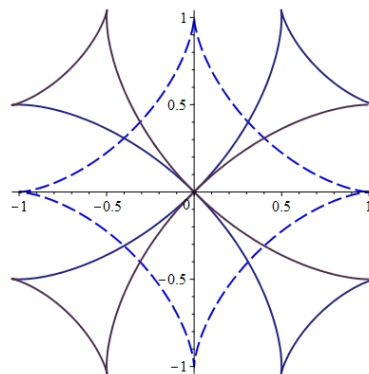


Figure 4: The astroid and the full envelope

Fig. 5 shows two snapshots of an animation (programmed with Maple 2020). Note that for every value of the parameter, the corresponding circle is tangent to both of the components determined by the parametrizations (4a) and (4b). For the reader's sake, we insert here the Maple code for the animation²:

```
with(plots):
ax := implicitplot({ x = 0, y = 0 }, x = -2 .. 2, y = -2 .. 2, color = black):
astr:= plot([cos(t)^3, sin(t)^3, t = 0 .. 2*Pi], color = blue):
```

²In order to run the animation, compile the Maple code, then right click on the plot. A bar of buttons to run the animation is then displayed. The author wishes to thank Maplesoft's support team for technical help, in order to remove superfluous components from the plot.

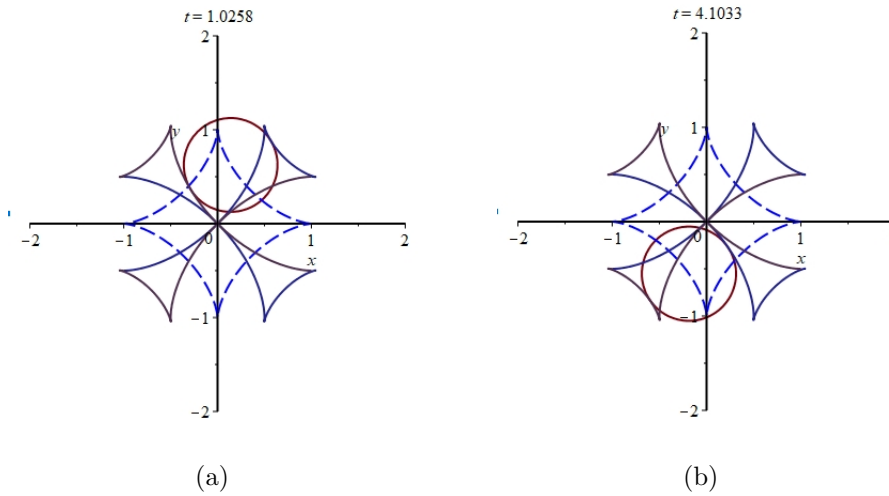


Figure 5: Animation snapshot: the astroid, the envelope and two circles

```
G := (x - cos(t) ^ 3) ^ 2 + (y - sin(t) ^ 3) ^ 2 - 1:
derG := diff(G, t):
paramenv := allvalues(solve({ G = 0, derG = 0 }, {x, y })):
env1 := plot([rhs(paramenv[1][1]), rhs(paramenv[1][2]), t = 0 .. 2*Pi-0.1], color = green):
env2 := plot([rhs(paramenv[2][1]), rhs(paramenv[2][2]), t = 0 .. 2*Pi-0.1], color = green):
circles := animate(implicitplot, [G = 0, x = -2 .. 2, y = -2 .. 2], t = 0 .. 2*Pi, frames = 50):
display(circles, env1, env2, astr, ax);
```

An interactive GeoGebra applet is available at <https://www.geogebra.org/m/x9mxfhph>. A screen snapshot of it is displayed in Fig. 6. Moving the point A along the astroid shows that the circle is tangent at one point to each of the components of the full envelope.

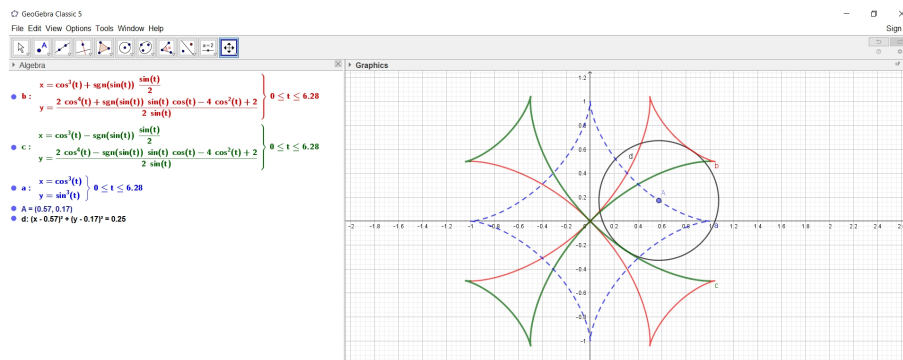


Figure 6: A screen snapshot of a GeoGebra applet

Another noticeable fact is that the union of the two components is a well known curve:

Proposition 7 *The envelope (according to Def. 1) of the given family of circles centred on the astroid is a Maltese Cross rotated counterclockwise by $\pi/4$.*

Ideas for a Proof: In the two first cases, we use the data provided by the Mathcurve site. Both ways are based on previous knowledge on classical curves, i.e. a visual recognition of a counterclockwise rotated copy of the Maltese cross by an angle of $\pi/4$.

First way - graphical checking: the website provides a parametric presentation for (half) a Maltese cross, whose symmetry axes are the coordinate axes, namely:

$$\begin{cases} x = \cos t (\cos^2 t - 2) \\ y = \sin t \cos^2 t \end{cases} \quad (8)$$

We apply the rotation about the origin by angle $\pi/4$, whose matrix is $\begin{pmatrix} \frac{\sqrt{2}}{2} & -\frac{\sqrt{2}}{2} \\ \frac{\sqrt{2}}{2} & \frac{\sqrt{2}}{2} \end{pmatrix}$, and obtain the following parametrization:

$$\begin{cases} x = \frac{\sqrt{2}}{2} (\cos t \cos^2 t - 2)/2 - \sin t \cos^2 t \\ y = \frac{\sqrt{2}}{2} (\cos t \cos^2 t - 2)/2 + \sin t \cos^2 t \end{cases} \quad (9)$$

Figure 7a shows both the original half Maltese Cross and the rotated one (dotted). Figure 7b shows a graphical check that the rotated Maltese Cross coincides with the envelope. Similar computations and checks have to be performed for the counterclockwise rotated by $3\pi/4$ curve.

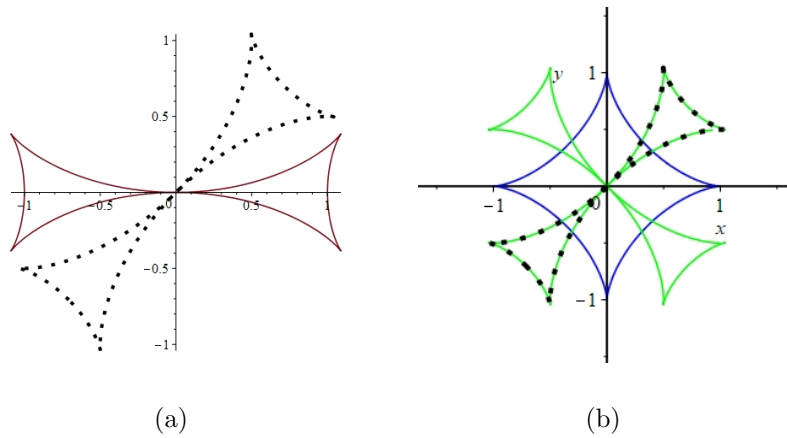


Figure 7: Half a Maltese cross and a rotated image

A graphical check can be performed to ensure that the rotated curves coincide with the envelope. Of course, this provides conviction using technology, not a proof. ■

Second way - verification: the website provides also an implicit equation for half a Maltese Cross, namely

$$(x^2 + y^2)^3 - x^2(x^2 + 20y^2) - 8y^2(y^2 + 2) = 0. \quad (10)$$

We use the above mentioned rotation to obtain an implicit equation for a South-West to North-East oriented half Maltese Cross, i.e. a loop included in quadrants (I) and (III) of the plane³. A

³We use the traditional counterclockwise numbering in roman numbers of the quadrants, starting with (I) for the domain given by $x \geq 0$ and $y \geq 0$

similar computation, with a rotation angle of $3\pi/4$, provides an implicit equation for a North-West to South-East Maltese Cross. By separate substitution of the expressions in Equations (6) and (7), we check that the envelope and the "full" Maltese Cross are identical. ■

Third way - synthetic proof: We look for an implicit equation for the envelope. Let us start with the parametrization given in Equations (6), for $t \in [0, \pi]$ (whence $\sin t \geq 0$):

$$\begin{cases} x = \cos^3 t + \frac{1}{2} \sin t \\ y = -\frac{1}{2\sin t} (4 \cos^2 t - \cos t (2 \cos^3 t + \sin t)) \end{cases} \quad (11)$$

We use the trigonometric-to-rational change described by Equations (22) in Appendix A, and replace sines and cosines by rational expressions, so we can write:

$$\begin{cases} x = \left(\frac{1-m^2}{1+m^2}\right)^3 + \frac{1}{2} \frac{2m}{1+m^2} \\ y = -\frac{1}{2} \frac{2m}{1+m^2} \left(4 \left(\frac{1-m^2}{1+m^2}\right)^2 - \frac{1-m^2}{1+m^2} \left(2 \left(\frac{1-m^2}{1+m^2}\right)^3 + \frac{2m}{1+m^2}\right)\right) \end{cases} \quad (12)$$

After simplification, we have:

$$\begin{cases} x = -\frac{(m^2-2m-1)(m^4+m^3-m+1)}{(m^2+1)^3} \\ y = \frac{-m^6-m^4+16m^3+m^2+1}{(2(m^2+1)^3)} \end{cases} \quad (13)$$

Multiplying in both equations by the denominator and transferring right hand side to the left hand side, we obtain the two polynomials:

$$\begin{cases} P_1(x, y) = x(m^2 + 1)^3 + (m^2 - 2m - 1)(m^4 + m^3 - m + 1) \\ P_2(x, y) = 2y(m^2 + 1)^3 + m^6 + m^4 - 16 * m^3 - m^2 - 1 \end{cases} \quad (14)$$

These polynomials generate an ideal $J = \langle P_1, P_2 \rangle$ in $\mathbb{R}[x, y, m]$. By elimination of the parameter m , we obtain an ideal $J_E = \langle F \rangle$ in $\mathbb{R}[x, y]$, where $F(x, y)$ is the polynomial given by:

$$\begin{aligned} F(x, y) = & 4x^6 + 12x^4y^2 + 12x^2y^4 + 4y^6 - 13x^4 - 36x^3y \\ & + 82x^2y^2 - 36xy^3 - 13y^4 + 32x^2 - 64xy + 32y^2. \end{aligned} \quad (15)$$

The variety $V(J_E)$ is the projection on the (x, y) -space of $V(J)$ in the (x, y, m) -space (see [10]). This variety is the component in quadrants (I) and (III) of the Maltese Cross displayed in Figure 4. A precise algebraic proof runs as follows: the subvariety $V(F_1)$ of the plane defined by the polynomial $F_1(x, y) = (x^2 + y^2)^3 - x^2(x^2 - 20y^2) - 8y^2(y^2 + 2)$ is the horizontal component of the "traditional" Maltese Cross (v.s. Equation (10)). Using the same rotation as above, we obtain the polynomial $F(x, y)$.

Starting now from the parametrization

$$\begin{cases} x = \cos^3 t + \frac{1}{2} \sin t \\ y = -\frac{1}{2\sin t} (4 \cos^2 t - \cos t (2 \cos^3 t + \sin t)) \end{cases} \quad (16)$$

and following the same process, we find a subvariety $V(G)$ of the plane, where $G(x, y)$ is the polynomial given as follows:

$$\begin{aligned} G(x, y) = & 4x^6 + 12x^4y^2 + 12x^2y^4 + 4y^6 - 13x^4 + 36x^3y \\ & + 82x^2y^2 + 36xy^3 - 13y^4 + 32x^2 + 64xy + 32y^2. \end{aligned} \quad (17)$$

Using now the inverse rotation, we obtain the equation of the component in quadrants (II) and (IV) of the envelope. All this can be checked graphically also.

For the reader's sake, we include here the Maple code that we used (we copy the formula for the initial trigonometric parametrization; they have been actually computed in a previous part of the Maple session).

```
with(PolynomialIdeals):
x[1] := cos(t)^3 + 1/2*sin(t):
y[1] := 1/(2*sin(t))*(2*cos(t)^4 - 4*cos(t)^2 + cos(t)*sin(t) + 2):
xrat[1] := simplify(subs(cos(t) = (-m^2 + 1)/(m^2 + 1), subs(sin(t) = 2*m/(m^2 + 1), x[1]])):
yrat[1] := simplify(subs(cos(t) = (-m^2 + 1)/(m^2 + 1), subs(sin(t) = 2*m/(m^2 + 1), y[1]])):
p1 := x*denom(xrat[1]) - numer(xrat[1]):
p2 := y*denom(yrat[1]) - numer(yrat[1]):
J:=< p1,p2 >:
JE := EliminationIdeal(J, x, y):
F := Generators(JE)[1]:
implicitplot(F = 0, x = -4 .. 4, y = -4 .. 4, numpoints = 5000);
```

The *PolynomialIdeals* package contains commands defining ideals and implementing algebraic algorithms, in particular the command we used to eliminate the variable m . The *numpoints* option in the last command is intended to have an accurate plot⁴.

4 An envelope delimiting a safety zone

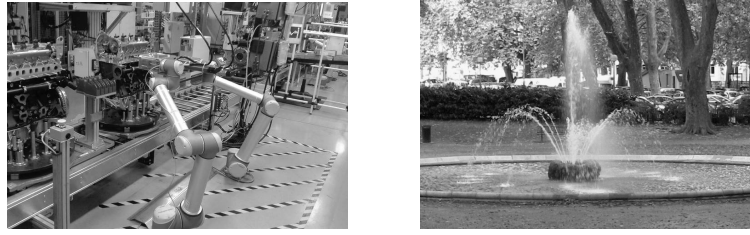
There is an important difference between envelopes of a given family of curves, according either to Def. 1 or to Def. 1, or to Def.5, in particular regarding possible physical meanings. Envelopes have applications in engineering and other domains (hydrology, soils, human safety around robots, etc.). For example, look at the marks on the floor in industrial plants where robots are working: the colored marks define the zones where human beings can safely walk. It is generally understood that these marks are determined by the envelopes of the trajectories of the robots and their mobile parts; see Fig. 8(a).

A more frequent example (in 3D) is given by a sprinkler: the envelope of the trajectories of water drops determines the frontier out of which you remain dry; see Fig. 8(b). This is explained in [15] and Def. 1 and Def. 4 have similar physical meanings. In real life, people will take some more distance in order to stay safe.

Back to our example, we consider the family of circles with radius $\frac{1}{2}$ centred on the astroid \mathcal{A} . Imagine a concrete realization of the astroid as a rail, on which circular "nests"⁵, where visitors can sit (and hopefully enjoy) can travel. The safety zone should be determined by what is displayed in Fig. 2 (of course, in a concrete construction, say for an amusement park, the safety zone would be probably defined a little farther from the mobile device. The safety zone according to Def. 4 is different from the envelope according to Def. 1; compare with Fig. 4. In order to explore which kind of curve is the frontier of the safety zone and the interior of the zone covered by the circles, and to derive an analytic description of it, we use technology again. We denote the curve we are looking for by \mathcal{H} .

⁴<https://www.maplesoft.com/support/help/Maple/view.aspx?path=plot/options>

⁵For a stronger feeling, the engineers could plan revolving nests, but this is irrelevant to our topic.



(a) Industrial plant

(b) Sprinkler

Figure 8: Safety zones

Remark 8 1. *The geometric situation presents numerous symmetries. Therefore, we conduct our exploration in the first quadrant only, i.e. for $0 \leq t \leq \frac{\pi}{2}$.*

2. *The exploration with the DGS will provide an approximation of the envelope, not an analytic answer.*

The general point $A(t)$ of \mathcal{A} has coordinates $(\cos^3 t, \sin^3 t)$, thus a tangent vector at $A(t)$ to the astroid has coordinates $(-3 \cos^2 t \sin t, 3 \sin^2 t \cos t)$. For $t = k\frac{\pi}{2}$, $k \in \mathbb{Z}$, this vector vanishes, whence the existence of 4 singular points, namely at coordinates $(1, 0), (0, 1), (-1, 0), (0, -1)$. At other points this tangent vector (we may eventually multiply it by $1/3$) is a direction vector of the tangent line, and a normal vector to the astroid at $A(t)$ has coordinates $(\sin^2 t \cos t, -\cos^2 t \sin t)$. An implicit equation for the normal line to \mathcal{A} at $A(t)$ is thus (after simplifications):

$$x \cos t - y \sin t + 1 - 2 \cos^2 t = 0. \tag{18}$$

The circle in the given family, centered at $A(t)$ has equation

$$(x - \cos^3 t)^2 + (y - \sin^3 t)^2 = \frac{1}{4}. \tag{19}$$

The normal line intersects the circle at two points, whose coordinates are functions of the parameter t ; the formulas are identical to Equations (11) (and similar to them for the other quadrants). Plotting according to these parametrizations yields exactly the curves displayed in Figure 3. This does not mean that the whole of the plot has to be considered. The previous study shows that not all of this offset can be considered as a part of the curve \mathcal{H} , but only some arcs. For symmetry reasons, we will study one arc, and especially, one endpoint of this arc.

The output of the geometric construction with normals is displayed in Figure 9: we obtain the four black arcs only, i.e. parts of the curves determined by the above parametrization are superfluous. Figure 10 shows two snapshots of an animated GIF, from a GeoGebra applet. We will see later that these black arcs are less simple than what appears at first glance.

A strong **Zoom in** has been used for Fig. 11: it reveals the different arcs when the parameter approaches $t = \pi/2$, i.e. when the point $A(t)$ is at the Northern cusp of the astroid, the DGS displays an "undefined" answer for several objects. On the left is an arc of the astroid (in blue), and on the right an arc of the offset. The point A is the center of the variable circle (plotted in orange). In order to have a better insight into what happens in this "tiny"

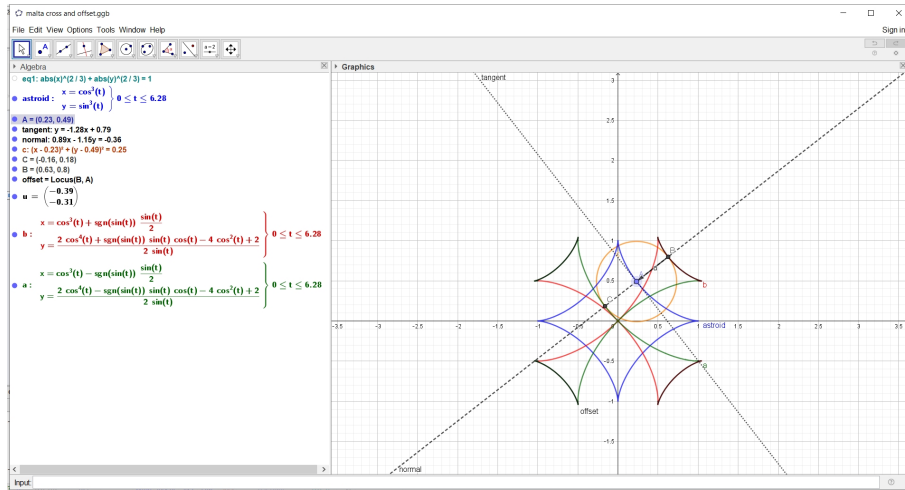


Figure 9: A GeoGebra session for the offset as defined with normals

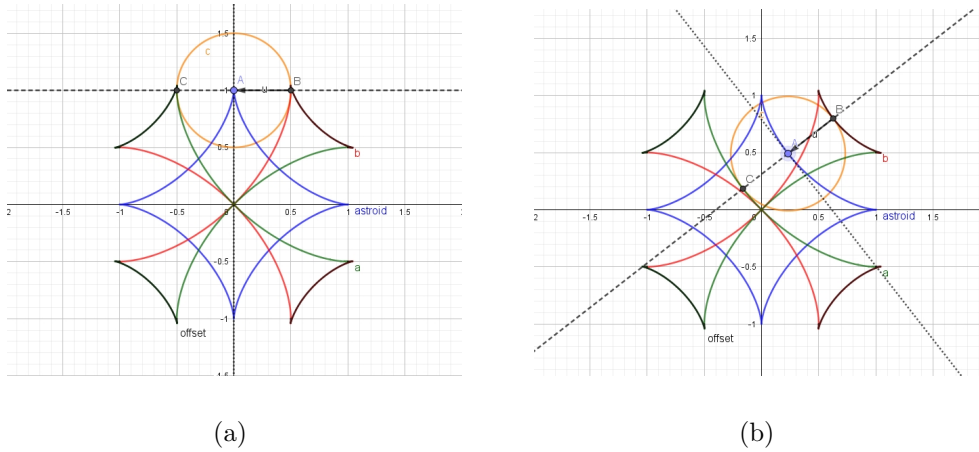


Figure 10: Second exploration of the frontier of the safety zone

area, we zoomed stronger and increased the precision of the numerical display, rounding to 5 decimal places⁶. Figure 12 shows an arc of the offset (in black), an arc of the variable circle (in orange) and an arc of the northernmost circle of the family, i.e. the unit circle whose center has coordinates (0, 1) (in green). Two points M and N are plotted on the offset and the northernmost circle respectively. An interactive check shows that the two curves intersect at point $P(0.49859, 1.03743)$. Pay attention that this is an approximation only⁷. Denote now this point by P_I . We denote by N' , N'' and N''' the images of the point $N = P_I$ by successive reflexions about the coordinate axes. Finally we have:

⁶The standard until now was 2 decimal places.

⁷On the one hand, it is reasonable to think that more digits after the decimal period will yield a more precise determination of the point of intersection of the offset and the circle. Nevertheless, as the central issue is to determine a safety zone, an engineer would work here with a lower precision, but put a fence much farther from the mobile installation than exactly the curve we are exploring. On the other hand, a CAS assisted solution of the exact equations is quite complicated. Its output involves the placeholder *RootOf*; the command **allvalues** do not yield exact solutions and **evalf** provides then approximated solutions.

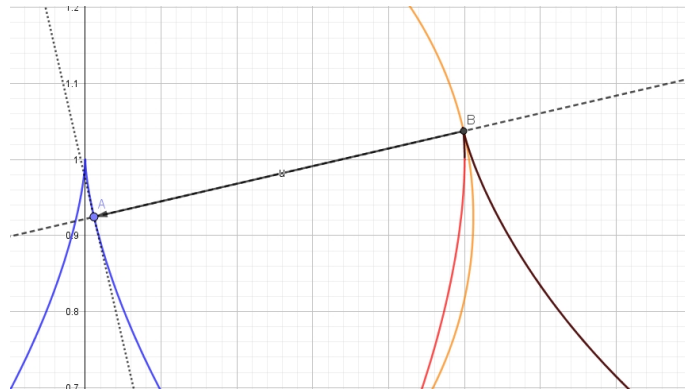


Figure 11: Behavior of the offset for t close to $\pi/2$

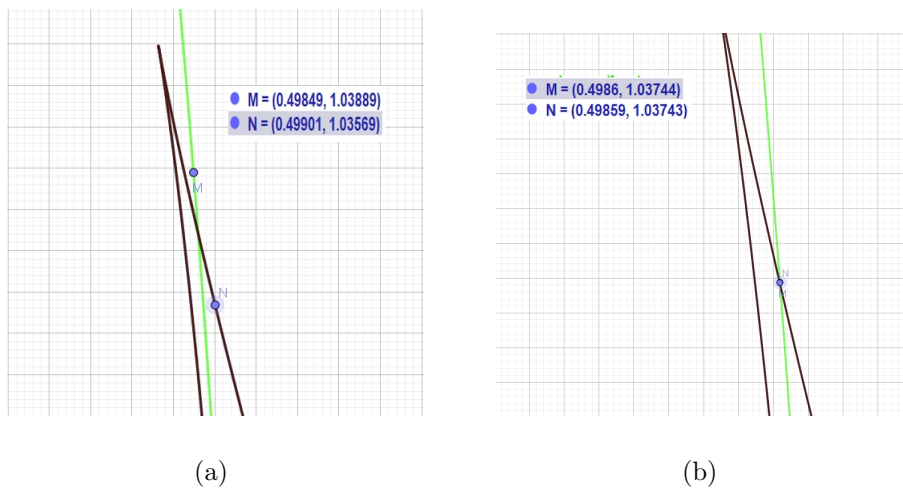


Figure 12: Exploration of the frontier of the safety zone close to a special point

Proposition 9 *The offset at distance $\frac{1}{2}$ of the astroid is the closed curve obtained as the union of the following arcs (see Figure 13; the safety line is in black):*

- *The arc NN' of the Maltese Cross and its images by successive reflexions about the axes⁸, i.e. arcs $N'N''$, $N''N'''$ and $N'''N$.*
- *The external arcs with the same endpoints on the northernmost, westernmost, southernmost and easternmost circles of the given family.*

Remark 10 *We should check whether the connection at N is smooth or not, i.e. whether the arc of the Maltese Cross and the arc of the circle have a common tangent at N or not. This can be checked using first order derivatives; anyway, here the answer can be approximated only.*

⁸These arcs are also the images of NN' by rotations about the origin by angles $\frac{k\pi}{2}$, $k = 1, 2, 3$

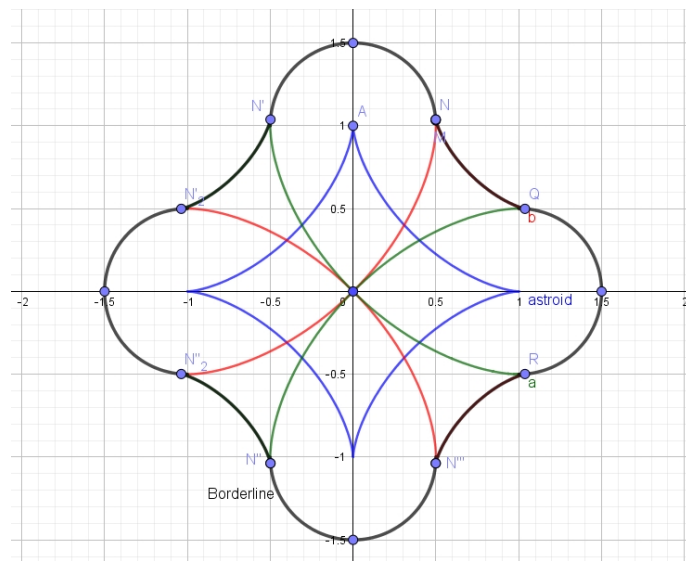


Figure 13: The borderline of the safety zone.

5 Discussion

We used a CAS and a DGS together. They have different strengths and different weaknesses, and their joint usage provided a broad insight into the study.

The first step was a DGS experimentation, providing a conjecture, but not a proof. Then, a parametrization of the envelope has been derived, and an animation has been built.

Animations with a CAS and with a DGS have different properties, in particular their interactivity is different. Both contribute to the insight into the problem under study. A CAS animation is generally programmed using existing commands, and is launched by "pressing a button" after having defined the number of frames per second. With a DGS, the interaction man-machine is more direct, commanded by the user's hand and the mouse. At some extent, the user can also act on the animation in real time, but not as much as with a DGS. A global picture of the astroid, some circles and the envelope(s), have been obtained by that joint work.

Zooming with the DGS re-computes the necessary data, when zooming-in with the CAS inflates the cells, but not re-compute data, and no new data is shown. This has been analyzed in [38]. The first plots could have been misleading, as it seemed that the point of contact between the northernmost circle and the eastern offset arc has coordinates $(1/2, 1)$. Only a strong zooming-in showed that it is not, and led to consider approximations of the coordinates with a higher degree of precision. A nice effect is that this zooming-in gives a feeling to "enter" into the picture. This zooming revealed also that the cusps on the astroid and on the offset do not correspond to the same values of the parameter.

Exploration of position and moves of the tangency points of the variable circle with the envelope(s) has been performed. Denote by \mathcal{E}_1 and \mathcal{E}_2 the curves determined by Equations (6) and (7). For every value of the parameter t , the corresponding circle is tangent at one point to \mathcal{E}_1 and at one point to \mathcal{E}_2 . This reinforces the understanding that each component \mathcal{E}_1 and \mathcal{E}_2 taken separately, is an envelope of the family.

The study of an offset has been made possible via a certain *dialog* between CAS and DGS, with a human being between them for copy-paste. Such a dialog is central in other studies

of curves and surfaces; see [14, 17]. Its contents depend on the mathematical domain. The development of CAS and DGS, and their joint influence, enabled to revive classical topics and to make new discoveries on classical curves. The state-of-the-art of the CAS-DGS dialog is analyzed in a subsequent paper [18], with a comparison of affordances of both kinds of software. We hope that, in the near future, this dialog will become more efficient, we mean automated.

When studying envelopes, it happens that the output includes non accurate components. This depends on the algorithms, which may return the desired envelope not as a projection of the variety V determined first in the (x, y, t) -space on the (x, y) -space but as its closure. The output is also dependent on how the family of curves has been given. These issues are addressed, with various examples, in [9]. An interesting comparison of the affordances of various packages is given there. We refer also to [26].

The main steps in the exploration of envelopes are the determination of a parametric presentation, then implicitization. Note that parametric presentation and implicit presentation do not show envelope components the same way, as we saw in Section 3.

Finally, we wish to emphasize that this kind of work is part of a long range vision, expressed by Monge (in [25], quoted by [24]: "Il faut donc que l'élève s'accoutume de bonne heure à sentir la correspondance qu'ont entre elles les opérations de l'analyse et celles de la géométrie ; il faut qu'il se mette en état, d'une part, de pouvoir écrire en analyse tous les mouvements qu'il peut concevoir dans l'espace, et, de l'autre, de se représenter perpétuellement dans l'espace le spectacle mouvant dont chacune des opérations analytiques est l'écriture."⁹

A Appendix: Rational expressions

The unit circle has a well known trigonometric parametrization given by

$$\begin{cases} x = \cos t \\ y = \sin t \end{cases}, t \in [0, 2\pi]. \quad (20)$$

Let $B(-1, 0)$ and L_m be the line through B with slope m . The line L_m intersects the unit circle at a second point B_m whose coordinates are

$$\begin{cases} x_m = \frac{1-m^2}{1+m^2} \\ y_m = \frac{2m}{1+m^2} \end{cases} \quad (21)$$

These formulae are a rational parametrization of the unit circle. Note that this parametrization does not include the point B itself. This is common for rational parametrizations, which are valid for "almost all" points of the given curve. Note also that if a rational parametrization exists, it is not unique. For a general study of rational curves with a CAS approach, we refer to [32]. An immediate consequence is that for every value of t , there exists a value of m such that

$$\begin{cases} \cos t = \frac{1-m^2}{1+m^2} \\ \sin t = \frac{2m}{1+m^2} \end{cases} \quad (22)$$

⁹Free translation: The student has to get used to feeling early the correspondence between the operations of the analysis and those of geometry; he has to put himself in a position, on the one hand, to be able to write an analysis of all the movements in space that he can imagine, and, on the other hand, to have perpetually a space representation of the moving spectacle, each of which analytical operations is a written description.

By substitution into Equations (2), we obtain a rational parametrization of the astroid \mathcal{A} :

$$\begin{cases} x = \left(\frac{1-m^2}{1+m^2}\right)^3 = \frac{(1-m^2)^3}{(1+m^2)^3} \\ y = \left(\frac{2m}{1+m^2}\right)^3 = \frac{8m^3}{(1+m^2)^3} \end{cases} \quad (23)$$

In what follows, we go back to the tradition and denote the parameter by t again.

Following the same process as in Section 3, we obtain rational parametrizations for two envelope components:

$$\begin{cases} x_1(t) = \frac{(t^2+2t-1)(t^4-t^3+t+1)}{(t^2+1)^3} \\ y_1(t) = \frac{t^6+t^4+16t^3-t^2-1}{2(t^2+1)^3} \end{cases} \quad \text{and} \quad \begin{cases} x_2(t) = \frac{(t^2-2t-1)(t^4+t^3-t+1)}{(t^2+1)^3} \\ y_2(t) = \frac{-t^6-t^4+16t^3+t^2+1}{2(t^2+1)^3} \end{cases} \quad (24)$$

whose plots are displayed in Figure 14. Note that in this case, each component is a loop with

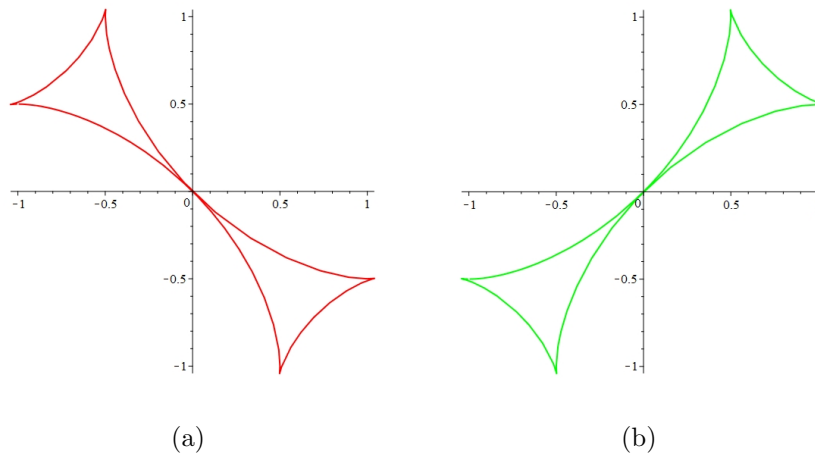


Figure 14: A new decomposition into two components of the envelope

cusps. Their union coincides in what is displayed in Figure 4. The algebraic method of Section 3 yields the same implicit equations and developments as Equation (10) and its consequences.

Now, why did we decide to work with the trigonometric and not with the rational parametrization? The answer lies in the animations (Fig. 5, 6 and 15). Compare the moves of the point in both animations: the trigonometric parametrization provides more regular moves than the rational one. With the last, moves are too slow, then too quick. The snapshots in Fig. 15 are part of an animated GIF of a Maple animation.

References

- [1] Abánades, M.A., Botana, F., Montes, A. and Recio, T., "An algebraic taxonomy for locus computation in dynamic geometry", *Computational Aided Design* **56**, 2014, 22–33.
- [2] Alcazar, J.G. and Sendra, J.R., "Local shape of offsets to algebraic curves", *Journal of Symbolic Computation* **42**, 2017, 338-351.

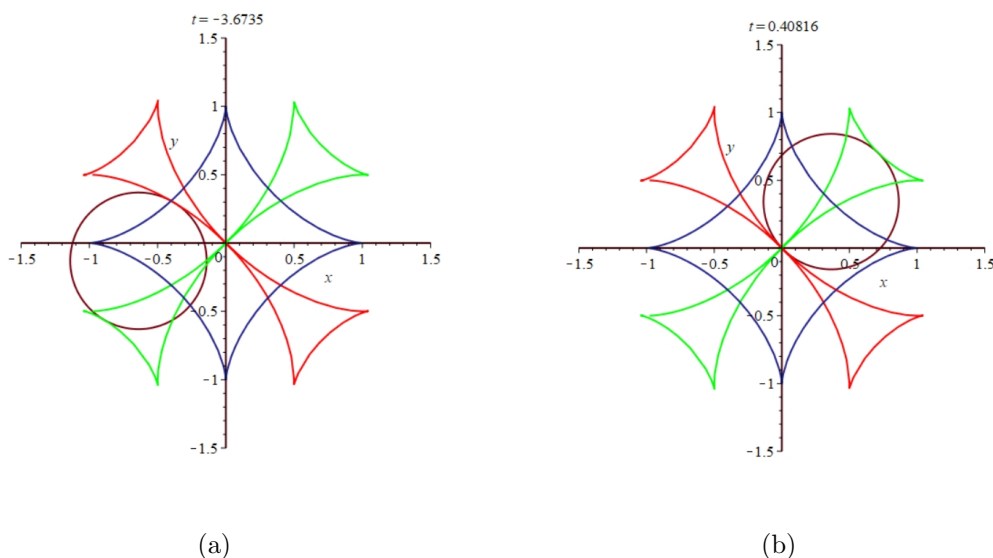


Figure 15: Animation snapshot: the astroid, the envelope and two circles

- [3] Berger, M. *Geometry*, Springer Verlag, 1994.
- [4] Blazek, J. and Pech, P., "Locus Computation in Dynamic Geometry Environment", *Mathematics in Computer Science* **13** (1-2), 2019, 31-40.
- [5] Botana, F. and Abánades, M.A., "Automatic deduction in (dynamic) geometry: Loci computation", *Computational Geometry* **47** (1), 2014, 75-89.
- [6] Botana, F., Valcarce, J., "A dynamic-symbolic interface for geometric theorem discovery", *Comput. Educ.* **38**, 2002, 21-35.
- [7] Botana, F. and Valcarce, J.L., "Automatic determination of envelopes and other derived curves within a graphic environment", *Mathematics and Computers in Simulation* **67**, 2004, 3-13.
- [8] Botana, F. and Recio, T., "Some issues on the automatic computation of plane envelopes in interactive environments", *Mathematics and Computers in Simulation* **125**, 2016, 115-125.
- [9] Botana, F. and Recio, T., Computing envelopes in dynamic geometry environments. *AMAI (Annals of Mathematics and Artificial Intelligence)* **80** (1), 2017, 3-20.
- [10] Botana, F. and Recio, T., "A proposal for the automatic computation of envelopes of families of plane curves", *Journal of Systems Science and Complexity* **32**(1), 2019, 150-157.
- [11] Cagnac, G. Ramis, E. and Commeau, J., *Nouveau cours de Mathématiques Spéciales*, Masson & Cie, Paris, 1965.

- [12] Cox, D., Little, J. and O’Shea, D., *Ideals, Varieties, and Algorithms: An Introduction to Computational Algebraic Geometry and Commutative Algebra*, Undergraduate Texts in Mathematics, Springer, 1992.
- [13] Dana-Picard, Th., The isoptics of an astroid, *Journal of Symbolic Computation* **97**, 2020, 56-68.
- [14] Dana-Picard, Th. and Mozgawa, W., ”Automated exploration of inner isoptics of an ellipse”, to appear in *Journal of Geometry* 111, 2020. <https://doi.org/10.1007/s00022-020-00546-3>
- [15] Dana-Picard, Th., and Zehavi, N., ”Revival of a classical topic in Differential Geometry: the exploration of envelopes in a computerized environment”, *International Journal of Mathematical Education in Science and Technology* **47**(6), 2016, 938-959.
- [16] Dana-Picard, Th. and Zehavi, N., Automated Study of Envelopes transition from 1-parameter to 2-parameter families of surfaces, *The Electronic Journal of Mathematics and Technology* **11** (3),2017, 147-160. *Printed version in the Journal of Research of Mathematics and Technology* **6** (2), 11-2.
- [17] Dana-Picard, Th., Naiman, A., Mozgawa, W. and Cieślak, V., ”Exploring the isoptics of Fermat curves in the affine plane using DGS and CAS”, *Mathematics and Computer Science* **14**, 2020, 45-67.
- [18] Dana-Picard, Th. and Kovács, Z., ”Networking of technologies: a dialog between CAS and DGS”, to appear in *electronic Journal of Mathematics and Technology* **14** (1).
- [19] Gueudet, Gh. and Trouche,L., ”Mathematics teacher education advanced methods: an example in dynamic geometry”, *ZDM Mathematics* **43**, 2011, 399–411.
- [20] Kock. A., ”Envelopes - notion and definiteness”, *Beiträge zur Algebra und Geometrie (Contributions to Algebra and Geometry)* **48**, 2007, 345-350.
- [21] Kovács, Z., ”Achievements and Challenges in Automatic Locus and Envelope Animations in Dynamic Geometry”, *Mathematics in Computer Science* **13**, 2019, 131–141.
- [22] Kovács, Z., and Parisse, B., ”Giac and GeoGebra–improved Gröbner basis computations”, In: *Computer Algebra and Polynomials, Lecture Notes in Computer Science* **8942**, 2015, 126–138.
- [23] Laborde, C., ”The use of new technologies as a vehicle for restructuring teachers’ mathematics”, In T. Conney & F. L. Lin (Eds.), *Making sense of mathematics teacher education*, 2011, 87–109. Dordrecht: Kluwer Academic Publishers.
- [24] Langevin, R., ”Geometry with two screens and computational graphics”, CAGIR 2014, downloadable: <http://math.uni.lodz.pl/~maczar/cagir/Langevin2014.pdf>, 2014.
- [25] Monge, G. *Leçons de géométrie descriptive*. Paris, Beudoin an VII (1798); re-edited by Jacques Gabay, Sceaux, France, 1989.

- [26] Montes, A. , *The Gröbner Cover*, Algorithms and Computations in Mathematics **27**, Springer, 2018.
- [27] Pottman, H. and Peternell, M., "Envelopes - Computational Theory and Applications". In: Proceedings of Spring Conference in Computer Graphic, Budmerice, Slovakia, 2000, 3-23.
- [28] Recio, T. and Vélez, M.P., "Automatic discovery of theorems in elementary geometry", *Journal of Automated Reasoning* **23**, 1999, 63–82.
- [29] San Segundo,F. and Sendra, J.R., "Degree formulae for offset curves", *Journal of Pure and Applied Algebra* **195**, 2005, 301-335.
- [30] San Segundo,F. , Sendra, J.R. (2009). "Partial degree formulae for plane offset curves", *Journal of Symbolic Computation* 44, 635-654.
- [31] Schultz, T. and Juttler, B., "Envelope computation in the plane by approximate implicitization", *Applicable Algebra in Engineering, Communication and Computing* **22** (4), 2011, 265-288.
- [32] Sendra, J.R., Winkler, F. and Perez-Diaz, S., *Rational Algebraic Curves: A Computer Algebra Approach*, Springer, 2008.
- [33] Tapp, K., *Differential Geometry of Curves and Surfaces*, Springer, Undergraduate Texts in Mathematics, 2016.
- [34] Thom, R., "Sur la théorie des enveloppes", *Journal de Mathématiques Pures et Appliquées* **XLI** (2),1962, 177-192.
- [35] Wu, W.T., "Some recent advances in mechanical theorem proving of geometries", in: W.W. Bledsoe, D.W. Loveland (Eds.), *Automated Theorem Proving: After 25 Years*, in: *Contemporary Mathematics* **29**, AMS, 235–241, 1984.
- [36] Wu, W.T., "Basic principles of mechanical theorem proving in geometries", *Journal of Automated Reasoning* **2**, 221–252, 1986.
- [37] Wu, W.T.: *Mechanical Theorem Proving in Geometries*, Springer, 1994.
- [38] Zeitoun, D. and Dana-Picard, Th., "On the usage of different coordinate systems for 3D plots of functions of two real variables", *Mathematics in Computer Science* **13**, 2019, 311-327.